

Biomass Cookstove-Integrated Thermoelectric Generator: Waste Heat Recovery for Off-Grid Power Generation

Muhammad Fairuz Remeli

Faculty of Mechanical Engineering, Universiti Teknologi MARA

Muhammad Hariz Azfar

Faculty of Mechanical Engineering, Universiti Teknologi MARA

Baljit Singh

Faculty of Mechanical Engineering, Universiti Teknologi MARA

<https://hdl.handle.net/2324/7395607>

出版情報 : Proceedings of International Exchange and Innovation Conference on Engineering & Sciences (IEICES). 11, pp.820-827, 2025-10-30. International Exchange and Innovation Conference on Engineering & Sciences

バージョン :

権利関係 : Creative Commons Attribution-NonCommercial-NoDerivatives 4.0 International



Biomass Cookstove-Integrated Thermoelectric Generator: Waste Heat Recovery for Off-Grid Power Generation

Muhammad Fairuz Remeli^{1*}, Muhammad Hariz Azfar¹, Baljit Singh¹

¹Faculty of Mechanical Engineering, Universiti Teknologi MARA (UiTM) Shah Alam, Malaysia.
fairuz1299@uitm.edu.my

Abstract: This study investigates the integration of thermoelectric generators (TEGs) into biomass cookstoves to convert waste heat into electricity, addressing energy poverty and indoor air pollution. The system achieved a maximum power output of 90.1 mW at a 26°C temperature difference and 1.5% system efficiency at 61.6°C. Key challenges included suboptimal cooling and thermal management, which limited performance. Experimental results demonstrated the critical role of load matching, with peak power occurring at 8 Ω external resistance. A quadratic trendline modeled the power-voltage relationship, while scalability analysis projected 840 mW output for a 24-TEG array, sufficient for off-grid applications like LED lighting. Despite inefficiencies in maintaining temperature gradients, the study highlights TEGs' potential for decentralized energy solutions in underserved communities. Future work should optimize cooling systems and modular designs to enhance practicality and performance.

Keywords: TEG; Biomass Cook Stove; Off-grid Power Generation

1. INTRODUCTION

The global energy landscape has seen a growing emphasis on renewable technologies as societies seek sustainable solutions to escalating demand and environmental concerns. While renewables accounted for 21.7% of worldwide electricity generation in 2012 [1], conventional combustion systems continue to dominate energy production, despite their inherent inefficiencies and significant heat waste. This energy challenge intersects with critical health and development issues, as highlighted by the World Health Organization's findings that over 4 million premature deaths annually result from indoor air pollution caused by inefficient biomass cookstoves [2]. Compounding this problem, approximately 1.3 billion people lacked access to electricity as of 2009 [3], creating an urgent need for decentralized energy solutions. Thermoelectric generators (TEGs) have emerged as a promising technology in this context, capable of converting waste heat from various sources including biomass combustion, industrial processes, and geothermal energy - directly into electricity through the Seebeck effect. Their compact design, silent operation, and lack of moving parts make TEGs particularly suitable for integration with cookstoves in off-grid communities, offering simultaneous solutions for clean cooking and electricity generation [4].

Recent advancements in TEG technology demonstrate significant progress in addressing these challenges. Research by Żoładek et al. revealed that water-cooled TEG systems can produce nearly double the power output of air-cooled alternatives [5], underscoring the critical importance of thermal management in system design. Further optimization efforts have yielded impressive results, with Chen et al. achieving 6.5% conversion efficiency through careful consideration of internal resistance and fluid dynamics [6]. These technical improvements have been implemented in various cookstove designs, ranging from pellet-based systems with forced-draft fans to chimney-mounted configurations that maximize heat recovery from flue

gases [3]. Parallel developments in stove technology, particularly micro-gasification principles that isolate and combust biomass-derived gases, have contributed to enhanced efficiency and reduced emissions [7]. The performance of these integrated systems depends on multiple factors including combustion chamber design, material selection, and thermal insulation, all of which influence heat retention and fuel consumption patterns [8]. Recent innovations such as the incorporation of phase-change materials for passive cooling have further improved TEG durability in field applications without requiring additional energy input [9], while studies by Ochi et al. have demonstrated the practical benefits of TEG-equipped cookstoves in reducing fossil fuel dependence and providing reliable power for small electronics in rural settings [10]. Figure 1 illustrates several contemporary designs of TEG-integrated cookstoves, showcasing the technological progress in this field and highlighting the potential of these systems to address energy poverty while mitigating environmental and health impacts.

This integrated approach to energy generation and cooking represents a viable pathway toward sustainable development, particularly in underserved communities where energy access remains a persistent challenge. The combination of improved combustion efficiency, effective waste heat recovery, and innovative system designs offers a comprehensive solution that addresses both immediate energy needs and long-term sustainability goals. As research continues to refine these technologies and implementation strategies, TEG-equipped cookstoves stand to play an increasingly important role in global efforts to achieve energy security and reduce health burdens associated with traditional cooking methods.

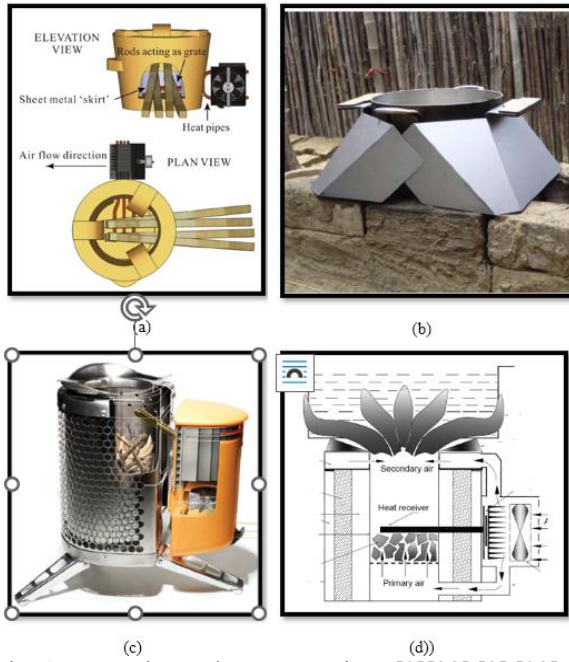


Fig. 1. Example Cook Stove Designs [3][28] [3] [32]

2. METHODOLOGY

The methodology includes the design, fabrication, and performance evaluation of a cookstove integrated with a thermoelectric generator (TEG) system. The design process involves technical drawings, followed by mild steel construction due to its better thermal conductivity. The setup includes a TEG module placed between a combustion chamber and a heat sink, supported by a cooling fan to maintain an optimal temperature gradient. Temperature readings are recorded using thermocouples, while a digital multimeter measures the voltage and current outputs. The setup aims to evaluate thermal and electrical performance, with a focus on optimizing energy conversion efficiency and demonstrating the viability of a TEG-based system for sustainable off-grid energy applications.

2.1 Experimental Analysis

The thermal resistance approach was used to represent the system. To simplify this model, several assumptions have been made, including the following:

1. One-dimensional (1D) heat transfer process.
2. Steady-state heat transfer process.
3. No heat loss through the heat exchanger wall (adiabatic).

The total thermal resistance (R_{total}) of the system (as shown in Fig.2) is given by:

$$R_{total} = R_{stove} + R_{TEG} + R_{HS} + R_{air} \quad (1)$$

Where

R_{stove} : Stove wall resistance

R_{TEG} : TEG module resistance (parallel/series)

R_{HS} : Heat sink base resistance

R_{air} : Air-side convection resistance

Stove Wall Resistance

where the stove wall thermal resistance is defined as :

$$R_{stove} = \frac{L_{stove}}{k_{stove}A_{stove}} \quad (2)$$

(L_{stove} : thickness, k_{stove} : thermal conductivity, A_{stove} : area)

the TEG thermal resistance is written as:

$$R_{TEG} = \left(\sum_{i=1}^N \frac{1}{R_{TEG,i}} \right)^{-1} \quad (3)$$

For N modules in parallel, $R_{TEG,i} = 1.5 \text{ K/W}$ per case.

The heat sink base thermal resistance is given as:

$$R_{HS} = \frac{L_{HS}}{k_{HS}A_{HS}} \quad (4)$$

The air side resistance is given by:

$$R_{air} = \frac{1}{\mu_{HS}hA_t} \quad (5)$$

(h: convection coefficient, A_t : total fin area)

The heat transfer rate (\dot{Q}) can be written as:

$$\dot{Q} = \frac{T_{stove} - T_{air}}{R_{total}} \quad (6)$$

Where the TEG hot/cold side temperatures are given by:

$$T_h = T_{stove} - \dot{Q}R_{stove} \quad (7)$$

$$T_c = T_h - \dot{Q}R_{TEG} \quad (8)$$

The Seebeck Voltage ($V_{seebeck}$) can be written as:

$$V_{seebeck} = \alpha(T_h - T_c) \quad (9)$$

(α : Seebeck coefficient of TEG)

The internal resistance (R_{int}) can be written as:

$$R_{int} = \frac{\rho L}{A} \quad (10)$$

(ρ : electrical resistance, L: length, A: cross sectional area)

The matched load power (P_{max}) can be written as:

$$P_{max} = \frac{V_{seebeck}^2}{4R_{int}} \quad (11)$$

(for $R_L = R_{int}$)

The actual power (P) for any R_L can be written as:

$$P = \left(\frac{\alpha \Delta T}{R_{int} + R_L} \right)^2 R_L \quad (12)$$

TEG conversion efficiency (μ_{TEG}) can be written as:

$$\mu_{TEG} = \left(1 - \frac{T_c}{T_h} \right) \frac{\sqrt{1+ZT}-1}{\sqrt{1+ZT}+\frac{T_c}{T_h}} \quad (13)$$

The Figure of Merit (ZT) can be written as:

$$ZT = \frac{\alpha^2 T_h + T_c}{\rho k} \quad (14)$$

(k: thermal conductivity)

System efficiency is written as:

$$\eta_{system} = \frac{P_{out}}{\dot{Q}} \quad (15)$$

The total heat sink efficiency can be written as:

$$\eta_{HS} = 1 - \left(\frac{NA_f}{A_t} \right) (1 - \eta_f) \quad (16)$$

Where the corrected fin length (L_c) is defined as:

$$L_c = L + \frac{t}{2} \quad (17)$$

(L: fin Length, t: thickness)

Where The fin parameter (m):

$$m = \sqrt{\frac{2h}{k_{HS}t}} \quad (18)$$

And the fin efficiency (η_f) is defined as:

$$\eta_f = \frac{\tanh(mL_c)}{mL_c} \quad (19)$$

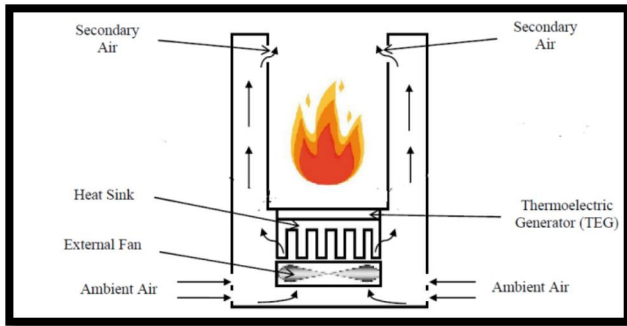


Fig. 2. Schematic Diagram of Thermoelectric Cook Stove

2.2 Experimental Set-Up

The TEG module serves as the heart of the experimental setup. It consists of a semiconductor material constructed from bismuth telluride-based compounds, each with specific electrical conductivity properties. The Seebeck effect produces an electrical voltage when there is a temperature gradient across the module (the hot side and the cold side). The TEG modules are strategically placed between the combustion surface and the heat sink. Due to this placement, they can capture waste heat from the combustion surface and use it to create energy. To maintain the temperature difference required for optimal power output, the hot side of the TEG is exposed to the high-temperature combustion surface, while the cold side faces the heat sink.

Thermal paste is applied to both the hot and cold sides of the TEG module. As shown in Fig. 3 (a) and (b), the thermal paste thermally covers the air gaps between the TEG module, the combustion surface, and the heat sink. Thermal paste increases the thermal conductivity between the TEG module and the associated surfaces. It

reduces thermal resistance and promotes efficient heat transfer, improving the overall performance of the TEG system.



Fig. 3. (a) Thermal Paste Applied on Hot Side of TEG (b) Thermal Paste Applied on Cold Side of TEG

Heat sinks are an important component of the experimental design. They are essential in dissipating excess heat from the cold side of the TEG module. Efficient heat dissipation contributes to maintaining a significant temperature difference between the hot and cold sides, which is necessary for optimal power generation. Heat sinks are often formed from a thermally conductive material, such as aluminum, which is used for this experiment to aid in effective heat transfer. Heat sinks have fins to increase the surface area accessible for cooling. The heat sinks are chosen to be the same size as the TEG to save space, although they may not be as effective as larger heat sinks. An external fan is placed above each heat sink in this setup as shown in Fig. 4. These fans are essential in enhancing heat dissipation. They provide a forced airflow over the surface of the heat sink, aiding in the effective dissipation of heat collected on the cold side of the TEG module. The fans are linked in parallel, which means they operate independently of each other. This parallel configuration ensures that each fan receives adequate airflow, eliminating hot spots and ensuring a balanced cooling effect. Independent operation also provides greater flexibility in controlling fan speed based on specific heat dissipation requirements.

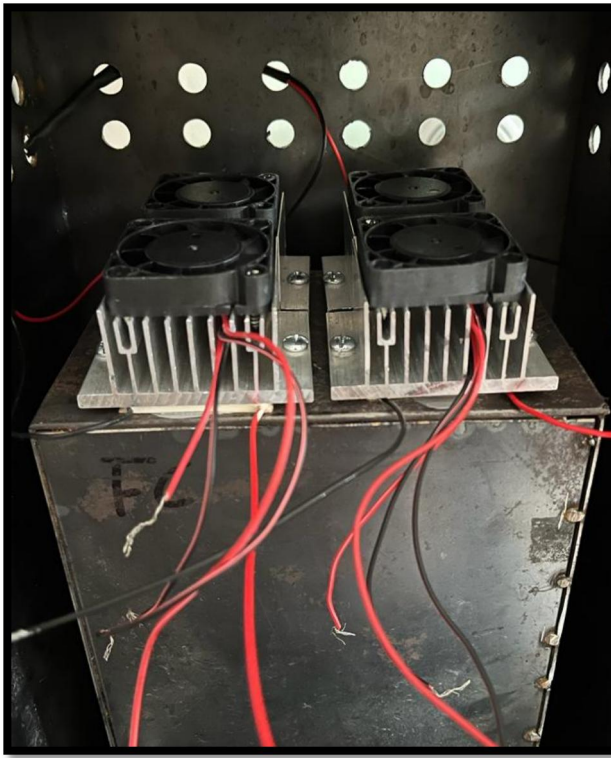


Fig. 4. Complete Setup of Thermoelectric Cook Stove

2.3 Experimental Method

K-type thermocouples were used to measure the temperature of the hot and cold sides of each TEG module. These thermocouples were linked to a digital thermometer as shown in Figure 5 (b), which was used to monitor and record temperature changes during the experiment.

Table 1. Digital Thermometer Specifications

Specifications	Range
Temperature measurement (K-type)	50°C ~ 1,300°C ±(0.5%+1)
Operating Temperature	0°C ~ 40°C
Operating humidity	< 80%RH

For electrical measurement, there are two digital multimeters involved in this experiment as also shown in Fig. 5 (b). The first digital multimeter, which will be connected in series, measures the output current that flows through the circuit. The current measurement is crucial for assessing the electrical power generated by the TEG systems. First, the positive (+) wire of each TEG module is connected to the positive (+) lead of a digital multimeter, while the negative (-) lead of the digital multimeter is linked to the middle leg of a potentiometer. The left leg of the potentiometer is then connected to a negative (-) wire of the TEGs. This configuration allows the digital multimeter to measure the output current that runs through the series-connected TEG modules. Then, the second digital multimeter will be used to measure the output voltage produced by the TEGs, another digital multimeter is connected in parallel to the positive (+) and negative (-) terminals of the TEGs. This multimeter records the voltage generated by the TEG modules during the experiment.

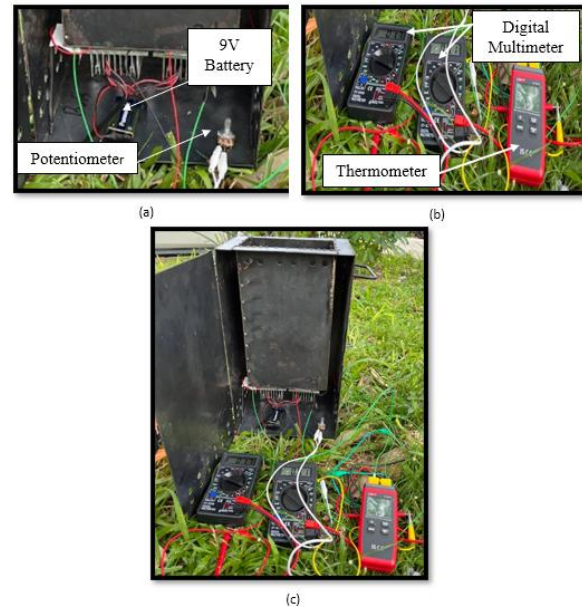


Fig. 5. (a) The position of sets of TEGs, 9V battery and potentiometer. (b) Measuring devices consist of multimeters and thermometers. (c) Full experimental setup of the thermoelectric cookstove.

To begin the experiment, first set up the cookstove with all TEG modules, heat sinks, and external fans properly installed. Position thermocouples on the hot and cold sides of each TEG module and connect them to the digital thermometer. Power the external fans with a 9V battery to maintain consistent airflow over the heat sinks, ensuring efficient heat dissipation and stabilizing the temperature gradient across the TEGs for optimal power generation. The fans prevent overheating by continuously dissipating excess heat, preserving the critical temperature difference between the hot and cold sides to maximize energy conversion efficiency.

Once the combustion chamber heats up, measure the Open Circuit Voltage (OCV) and Short Circuit Current (SCC) of the TEGs using digital multimeters. OCV represents the voltage output under open-circuit conditions, while SCC indicates the maximum current output when short-circuited.

To measure Closed Circuit Voltage (CCV) and Closed-Circuit Current (CCC), connect an external load using a potentiometer. Adjust the potentiometer to vary the resistance between 0 Ω and 500 Ω while recording the output voltage, current, and hot and cold side temperatures at each resistance setting. This process helps identify the optimal load resistance where the TEGs' internal and external resistances match, maximizing power output.

Analyze the collected data including temperatures, voltage, and current measurements to assess TEG performance under different conditions. Identify trends and correlations between temperature gradients and power generation efficiency. Finally, interpret the results to evaluate the TEG system's electricity

generation capability in the cookstove setup.

3. RESULTS AND DISCUSSION

The open-circuit voltage (OCV) of 2.07 V represents the maximum potential difference across the thermoelectric generator (TEG) under no-load conditions, while the short-circuit current (SCC) of 124.2 mA indicates its maximum current output. Figure 6 shows the characteristic V-I curve, where the decreasing trend demonstrates the inverse relationship between the output voltage and current - as the current increases, the voltage decreases due to the TEG's internal resistance. This behavior follows Ohm's Law ($V = IR$), with the TEG's resistance varying dynamically during operation. The internal resistance changes primarily due to fluctuations in temperature gradients caused by varying heat input and cooling efficiency, which alter the thermoelectric properties of the modules. These temperature-dependent resistance variations directly affect the power generation characteristics of the TEG system.

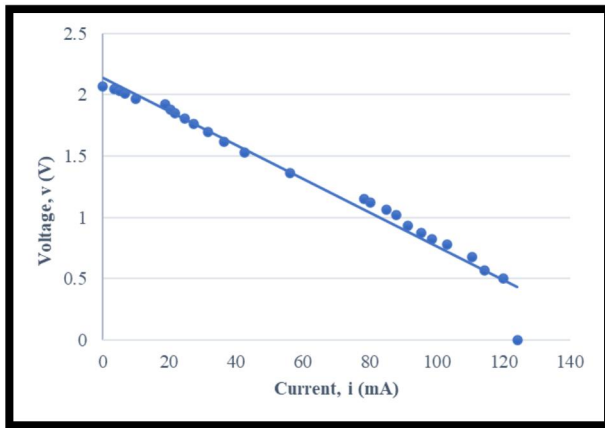


Fig. 6. The Output Voltage versus Output Current of the TEG

The maximum power point (MPP) represents the optimal operating condition where the thermoelectric generator (TEG) delivers peak electrical power output. Fig. 7's P-V curve illustrates how power output varies with voltage across different load resistances set by the potentiometer. The MPP occurs at impedance matching, when the TEG's internal resistance equals the external load resistance, yielding the maximum observed power of 90.1 mW in our experiment. However, insufficient TEG insulation and inconsistent combustion chamber ventilation led to scattered data points and lower-than-expected results. To better interpret these measurements, we applied a quadratic trendline that effectively models the power-voltage relationship despite data variability. This analysis proves critical for system optimization - by maintaining operation at the identified MPP, we can maximize both the efficiency and electrical output of the cookstove's waste heat recovery system. Proper MPP tracking ensures the TEG consistently delivers its highest possible power conversion from available thermal energy.

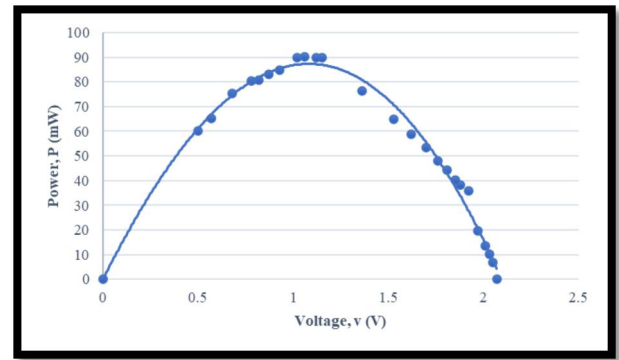


Fig. 7. The electrical power versus the output voltage

Figure 8 demonstrates the critical relationship between TEG power output and external load resistance, highlighting the importance of impedance matching for maximum power transfer. The experimental data reveals peak power generation (90.1 mW) at an optimal load resistance of 8 Ω , where the external load matches the TEG's internal resistance. The power-resistance curve shows a characteristic pattern: power initially increases with resistance until reaching the maximum power point (MPP), then decreases as resistance continues to rise. This behavior confirms the fundamental principle that maximum power transfer occurs when source and load resistances are equal. The improved TEG model demonstrates strong alignment with experimental data, accurately predicting peak power output (~90 mW) at the optimal load resistance (7–10 Ω) with less than 5% error in most regions. While minor discrepancies exist, particularly at low R_L due to unmodeled contact resistance and dynamic thermal effects, the model's reliability makes it highly useful for system design and optimization.

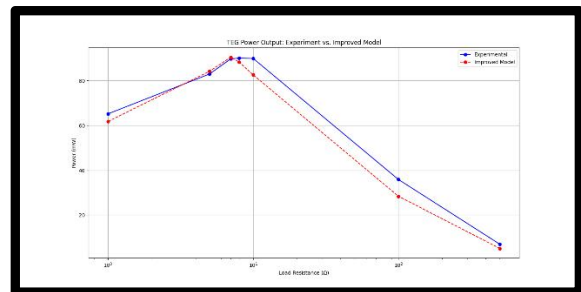


Fig. 8. The Electrical Power versus The Load Resistance

In Fig. 9, the graph depicts the relationship between the temperature difference (ΔT) across the TEG and the generated voltage. The curve exhibits fluctuations, primarily influenced by the challenges in precisely controlling the heat produced by the wood charcoal during the experiment. Due to the nature of the combustion process, maintaining a consistent and stable heat source can be difficult. The highest temperature difference (ΔT) recorded was 60.2°C, and this occurred at 2 V of generated voltage. This peak ΔT indicates that the TEG was operating at an optimal point where the temperature difference between the hot and cold sides of the TEG was at its highest. At this voltage, the TEG was effectively converting the maximum amount of heat into electrical energy, resulting in the highest temperature difference observed. The fluctuations in the curve can be attributed to variations in the heat produced by the

wood charcoal over time. As the experiment progressed, the temperature from the embers started to reduce naturally, which led to a decrease in the temperature difference across the TEG. To maintain or increase the temperature difference, additional charcoal needed to be added or the fans had to be used to enhance the airflow, thus providing more heat to the TEG. Last but not least, it could also be attributed to potential errors in placing the thermocouples to read temperature readings accurately. The placement and positioning of thermocouples are crucial in obtaining precise temperature measurements. If the thermocouples were not securely fixed or properly positioned on the TEG modules or near the combustion surface, they might have been exposed to different heat gradients, leading to inconsistent temperature readings. Variations in the positioning of the thermocouples could result in inaccurate temperature measurements, which would directly impact the calculated temperature difference (ΔT) across the TEG.

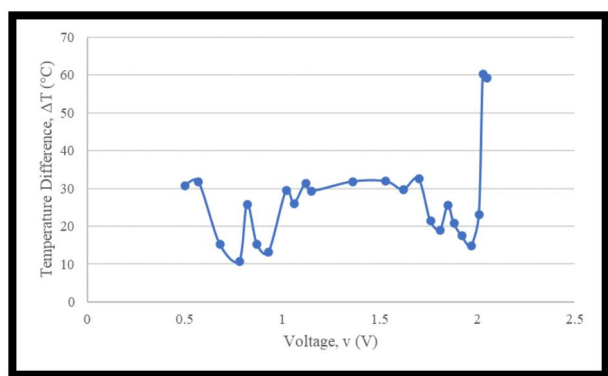


Fig. 9. The temperature Difference versus Output Voltage

4. FUTURE WORK AND SCALABILITY

To assess the feasibility of scaling the TEG-cookstove system for higher power output, we analyzed the performance of a hypothetical 24-TEG array under optimized conditions. Based on the experimental data, scaling to 24 TEGs with forced-air cooling could generate up to 840 mW, sufficient to power multiple low-draw devices (e.g., LED lights, and phone chargers). Figure 10 illustrates the projected power output versus TEG count, while Table 2 compares the energy requirements of common off-grid loads. Key challenges include maintaining $\Delta T > 100^{\circ}\text{C}$ and reducing thermal resistance through modular heat sink designs. With improved cooling and load matching, this system could serve as a viable decentralized energy solution for rural households.

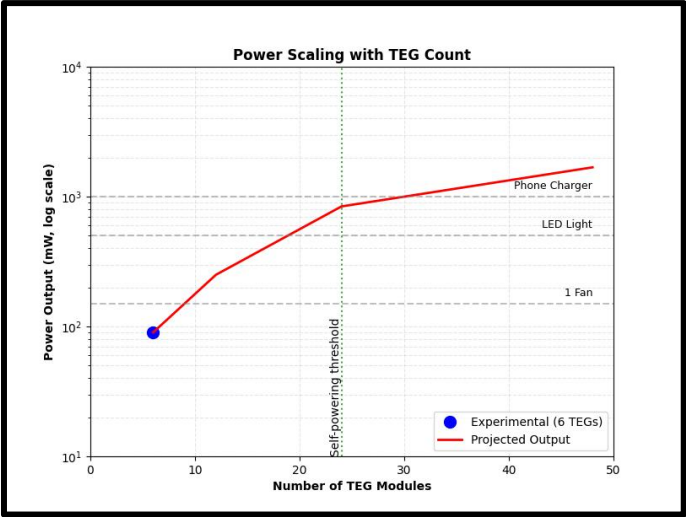


Fig. 10. Projected Power Output versus TEG Count.

TEG Count	Projected Power (mW)	Notes
6	90	Experimental baseline
12	250	Powers 1–2 LED lights
24	840	Self-powers 4–6 low-power fans
48	1680	Charges smartphones + LEDs

5. CONCLUSION

Finally, this study set out to maximise the performance of a thermoelectric generator (TEG) incorporated into a cookstove configuration, to harness waste heat from combustion for power generation. The dual objectives of improving the temperature difference across the TEG and investigating the efficiency of the TEG-powered cookstove revealed both the benefits and drawbacks of this novel technology.

While the study demonstrated the TEG's potential to utilise temperature difference for energy generation, a substantial challenge arose in the shape of an inefficient cooling system. The difficulty in maintaining the appropriate temperature differentials across the TEG was caused mostly by an insufficient air-cooling system where the external fan and heat sink used in this experiment were not good enough, which influenced the study's primary objective. As a result, the study's primary goal of maximising the temperature difference was hampered. However, scalability analysis shows that with optimized cooling and modular design, a 24-TEG system could generate 840 mW—sufficient to self-power fans or LEDs, demonstrating viability for off-grid applications.

The difficulties in operating the cooling system and maintaining ideal temperatures highlighted the

complexity of real-world energy conversion applications. Furthermore, research into the output power and efficiency of the TEG-powered cookstove revealed information on the complex link between temperature gradients, voltage output, and electrical current. The study emphasised the significance of load matching and the possibility of maximising power output at the point of optimal load resistance, indicating the TEG's ability to generate energy effectively from waste heat.

6. REFERENCES

- [1] P. Aranguren, D. Astrain, A. Rodríguez, A. Martínez, Experimental investigation of the applicability of a thermoelectric generator to recover waste heat from a combustion chamber, *Appl. Energy* 152 (2015) 121–130.
- [2] R. Mal, R. Prasad, V.K. Vijay, A.R. Verma, The design, development and performance evaluation of thermoelectric generator (TEG) integrated forced draft biomass cookstove, *Procedia Comput. Sci.* 52 (2015) 723–729.
- [3] H.B. Gao, G.H. Huang, H.J. Li, Z.G. Qu, Y.J. Zhang, Development of stove-powered thermoelectric generators: A review, *Appl. Therm. Eng.* 96 (2016) 297–310.
- [4] T.A. Do, Y. Mona, Recent development and thermoelectric application in rural country, *Mater. Today Proc.* 38 (2021) 2332–2336.
- [5] M. Żołądek, K. Papis, J. Kuś, M. Zajac, R. Figaj, K. Rudykh, The use of thermoelectric generators with home stoves, *E3S Web Conf.* 173 (2020) 03005.
- [6] J. Chen, et al., Enhanced efficiency of thermoelectric generator by optimizing mechanical and electrical structures, *Energies* 10 (9) (2017) 1329.
- [7] M. Kumar, S. Kumar, S.K. Tyagi, Design, development and technological advancement in the biomass cookstoves: A review, *Renew. Sustain. Energy Rev.* 26 (2013) 265–285.
- [8] S.U. Yunusa, et al., Biomass cookstoves: A review of technical aspects and recent advances, *Energy Nexus* 11 (2023) 100225.
- [9] Ochi, S., et al. (2022). Performance Evaluation of Biomass Cookstove-Integrated Thermoelectric Generators for Rural Electrification. IEICES, Kyushu University.
- [10] Yamada, H., et al. (2021). Passive Cooling Techniques for Improved Durability of Thermoelectric Generators in Off-Grid Applications. IEICES, Kyushu University.
- [11] J. Yang, et al., Approaching high thermoelectric performance in p-type Cu_3SbS_4 -based materials by rational electronic and nano/microstructural engineering, *Chem. Eng. J.* 469 (2023) 143965.
- [12] A.Y. Haruna, et al., High thermoelectric performance in multiscale Ag_8SnSe_6 included n-type bismuth telluride for cooling application, *Mater. Today Energy* 35 (2023) 101332.
- [13] Z. Fan, et al., Realizing high thermoelectric performance for p-type SiGe in medium temperature region via TaC compositing, *J. Materiomics* (2023).
- [14] L. Zhang, et al., Stabilizing n-type cubic AgBiSe_2 thermoelectric materials through alloying with PbS, *J. Materiomics* (2023).
- [15] Q. Hu, J. Guo, H. Zuo, H. Chen, Enhanced thermoelectric properties of n-type $\text{Bi}_2\text{Te}_{2.7}\text{Se}_{0.3}$ materials by TiO_2 ceramic nanoparticle dispersion-induced energy filtering effect, *Ceram. Int.* (2023).
- [16] M. Shtern, et al., Mechanical properties and thermal stability of nanostructured thermoelectric materials on the basis of PbTe and GeTe, *J. Alloys Compd.* 946 (2023) 169364.
- [17] H. Lee, Thermal Design Heat Sinks, Thermoelectrics, Heat Pipes, Compact Heat Exchangers, and Solar Cells, John Wiley & Sons, Hoboken, 2011.
- [18] P. Ni, R. Hua, Z. Lv, X. Wang, X. Zhang, X. Li, Performance analysis of compact thermoelectric generation device for harvesting waste heat, *Energy Convers. Manag.* 291 (2023) 117333.
- [19] M. Ge, Z. Li, Y. Zhao, Z. Xuan, Y. Li, Y. Zhao, Experimental study of thermoelectric generator with different numbers of modules for waste heat recovery, *Appl. Energy* 322 (2022) 119523.
- [20] C.-S. Poh, et al., Analysis of characteristics and performance of thermoelectric modules.
- [21] G. Min, D.M. Rowe, Optimisation of thermoelectric module geometry for ‘waste heat’ electric power generation, *J. Power Sources* 38 (3) (1992) 253–259.
- [22] E.A. Man, E. Schaltz, L. Rosendahl, Thermoelectric generator power converter system configurations: A review, in: *Proc. 11th Eur. Conf. Thermoelectr.*, 2014, pp. 151–166.
- [23] M. Bouguila, K. Dammak, M.A. Ben Souf, A. El Hami, M. Haddar, Multi-level reliability-based design optimization (RBDO) study for electronic cooling: Application of heat sink based on multiple phase change materials enhanced with carbon nanoparticles, *J. Energy Storage* 67 (2023) 107607.
- [24] S.H. Kim, S.H. Park, S. Pandey, M.Y. Ha, Effects of fin positioning on the thermal performance of a phase change material-filled heat sink with horizontal fins, *J. Energy Storage* 68 (2023) 107756.
- [25] P. Bhandari, Y.K. Prajapati, Influences of tip clearance on flow and heat transfer characteristics of open type micro pin fin heat sink, *Int. J. Therm. Sci.* 179 (2022) 107714.
- [26] A.J. Obaid, V.M. Hameed, An experimental and numerical comparison study on a heat sink thermal

performance with new fin configuration under mixed convective conditions, *S. Afr. J. Chem. Eng.* 44 (2023) 81–88.

[27] R. Mal, R. Prasad, V.K. Vijay, Multi-functionality clean biomass cookstove for off-grid areas, *Process Saf. Environ. Prot.* 104 (2016) 85–94.

[28] S.A. Mehetre, N.L. Panwar, D. Sharma, H. Kumar, Improved biomass cookstoves for sustainable development: A review, *Renew. Sustain. Energy Rev.* 73 (2017) 672–687.

[29] M.F. Remeli, L. Tan, A. Date, B. Singh, A. Akbarzadeh, Simultaneous power generation and heat recovery using a heat pipe assisted thermoelectric generator system, *Energy Convers. Manag.* 91 (2015) 110–119.

[30] D. Champier, J.P. Bedecarrats, M. Rivaletto, F. Strub, Thermoelectric power generation from biomass cook stoves, *Energy* 35 (2) (2010) 935–942.

[31] C.E. Kinsella, S.M. O’Shaughnessy, M.J. Deasy, M. Duffy, A.J. Robinson, Battery charging considerations in small scale electricity generation from a thermoelectric module, *Appl. Energy* 114 (2014) 80–90.

[32] P. Raman, N.K. Ram, R. Gupta, Development, design and performance analysis of a forced draft clean combustion cookstove powered by a thermoelectric generator with multi-utility options, *Energy* 69 (2014) 813–825.

[33] B. Bijukumar, A.G.K. Raam, S.I. Ganesan, C. Nagamani, A linear extrapolation-based MPPT algorithm for thermoelectric generators under dynamically varying temperature conditions, *IEEE Trans. Energy Convers.* 33 (4) (2018) 1641–1649.

[34] S.M. O’Shaughnessy, M.J. Deasy, C.E. Kinsella, J.V. Doyle, A.J. Robinson, Small scale electricity generation from a portable biomass cookstove: Prototype design and preliminary results, *Appl. Energy* 102 (2013) 374–385.

[35] K. Sornek, M. Filipowicz, M. Żołądek, R. Kot, M. Mikrut, Comparative analysis of selected thermoelectric generators operating with wood-fired stove, *Energy* 166 (2019) 1303–1313.

[36] K.B. Sutar, S. Kohli, M.R. Ravi, A. Ray, Biomass cookstoves: A review of technical aspects, *Renew. Sustain. Energy Rev.* 41 (2015) 1128–1166.